

General Label-free Fluorescent Aptamer Binding Assay Using Cationic Conjugated Polymers

Pengbo Zhang,^{ab} Ke Qin,^a Anand Lopez,^b Zhengping Li,^{*a} Juewen Liu^{*b}

^aSchool of Chemistry and Biological Engineering, University of Science and Technology Beijing, 30 Xueyuan Road, Haidian District, Beijing, 100083, China

^bDepartment of Chemistry, Waterloo Institute for Nanotechnology, University of Waterloo, 200 University Avenue West, Waterloo, Ontario N2L 3G1, Canada.

ABSTRACT: With more and more new aptamers being reported, a general, cost-effective yet reliable aptamer binding assay is still needed. Herein, we studied cationic conjugated polymer (CCP)-based binding assays taking advantage of the conformational change of aptamer after binding with a target, which is reflected by the fluorescence change of the CCP. Poly(3-(3'-N,N,N-triethylamino-1'-propyloxy)-4-methyl-2,5-thiophene hydrochloride) (PMNT) was used as a model CCP in this study and the optimal buffer was close to physiological conditions with 100 mM NaCl and 10 mM MgCl₂. We characterized four aptamers for K⁺, adenosine, cortisol and caffeine, respectively. For cortisol and caffeine, the drop in the 580 nm peak intensity was used for quantification, whereas for K⁺ and adenosine, the fluorescence ratio at 580 nm over 530 nm was used. The longer stem of stem-loop structured aptamer facilitated the binding of target and enlarged the detection signal. High specificity was achieved in differentiating target with analogues. Compared with the SYBR Green I dye-based staining method, our method achieved equal or even higher sensitivity. Therefore, this assay is practicable as a general aptamer binding assay. The simple, label-free, quick response and cost-effective features will make it a useful method to evaluate aptamer binding. At the same time, this system can also serve as label-free biosensors for target detection.

INTRODUCTION

With the development of systematic evolution of ligands by exponential enrichment (SELEX),^{1,2} more and more aptamers were selected to bind a wide range of targets, including metal ions, small molecules, peptides, proteins and even cells.³⁻⁶ Aptamers are low cost, highly stable, easy to modify and can undergo several cycles of denaturation and renaturation without affecting the binding ability.⁷ However, recent reports showed that many aptamers cannot bind to the intended targets and part of the problem lies in binding assays.⁸⁻¹¹ A key challenge in this field is to develop simple and effective methods to evaluate aptamer binding, especially for small molecules.¹²

Isothermal titration calorimetry (ITC) has been widely used to validate aptamers through monitoring the heat of binding.¹³ ITC is attractive as a label-free and highly accurate method, but the instrument is expensive and it is a low throughput technique. Many DNA intercalating dyes, such as SYBR Green I (SGI) and thioflavin T (ThT), have also been used.^{14,15} The conformational change of aptamers after target binding can either promote dye binding or displace dye molecules, resulting in a fluorescence intensity change.^{16,17} However, these label-free biosensors show relatively low fluorescence change due to the non-canonical structures of aptamers. Strategies using terminal labeled fluorophore and quencher pairs to form aptamer beacons were also employed.^{18,19} However, this method is quite expensive and the signal is often turned off upon target binding. Li and coworkers developed a general structure-switching strategy through the competition of a quencher-labeled complementary DNA (cDNA).²⁰ The binding of target molecules released the cDNA, leading to fluorescence recovery.^{21,22} This is a reliable method, although the cost of synthesis is still very high. Many

other fluorescence-based methods were also developed but they were not widely used.²³⁻²⁶

Using gold nanoparticles (AuNPs) to develop label-free colorimetric biosensors has been extensively investigated owing to its simplicity.²⁷⁻²⁹ This method relies on the differed binding affinities and kinetics of AuNPs towards single-stranded DNA (ssDNA) and well-folded or double-stranded DNA (dsDNA), and target-bound aptamers were believed to adsorb more slowly to AuNPs.³⁰⁻³² However, recent studies showed that many of the assays actually reflected target adsorption to AuNPs instead of aptamer binding to target molecules.³³ Thus, a general, simple and cost-effective binding assay is still needed.

Water-soluble cationic conjugated polymers (CCPs) have been widely used as probes for developing sensors due to their excellent optical properties.^{34,35} One strategy is to use a covalently labeled aptamer to measure the fluorescence resonance energy transfer (FRET) with a CCP.^{36,37} Label-free strategies were also attempted. For example, guanine-rich aptamers can form G-quadruplex in the presence of K⁺ or α -thrombin. Thymine-rich aptamers can fold DNA into a duplex through thymine-Hg²⁺-thymine interactions. Both reactions led to a conformational change of a CCP, resulting in a color or fluorescence change.^{38,39} DNA hybridization can also be probed by CCP.^{40,41} However, this method has only been applied in limited cases, such as the detection of metal ions or proteins. No work was performed on small molecule binding aptamers, which are a major aptamer type. In addition, no quantitative measurements were performed to evaluate it as a binding assay.

In this paper, we focused on using CCP to develop a label-free fluorescent binding assay. To investigate the generality, our

method was utilized to study a variety of aptamer targets including K^+ , adenosine, cortisol and caffeine. Although the four targets differed a lot in size, charge and hydrophobicity, all of them can induced fluorescence change of CCP within seconds at room temperature.

EXPERIMENTAL SECTION

Chemicals. The aptamers used in this work were purchased from Integrated DNA Technologies (Coralville, IA, USA). The sequences of aptamers are listed in Table S1. Lithium chloride (LiCl), rubidium chloride (RbCl), cesium chloride (CsCl), adenosine monophosphate (AMP), adenosine diphosphate (ADP), adenosine triphosphate (ATP), cortisol, thymidine, β -estradiol, deoxycholic acid, dopamine, caffeine, paraxanthine, theobromine, theophylline, ThT, SGI and hydrochloric acid were from Sigma-Aldrich. Sodium chloride (NaCl), potassium chloride (KCl), magnesium chloride ($MgCl_2$), sodium phosphate monobasic anhydrous (NaH_2PO_4), sodium phosphate dibasic (Na_2HPO_4), adenosine, guanosine, cytidine, uridine, 4-(2-hydroxyethyl) piperazine-1-ethanesulfonic acid (HEPES) and tris(hydroxymethyl)aminomethane (Tris) were from Mandel Scientific (Guelph, ON, Canada). Poly(3-(3'-N,N,N-triethylamino-1'-propyloxy)-4-methyl-2,5-thiophene hydrochloride) (PMNT) was customized from Okeanos Tech. Co., Ltd using the method depicted in previous papers.^{40, 42} Milli-Q water was utilized for preparing all the buffers and solutions.

K^+ binding assays. A typical reaction had a volume of 100 μ L. In a 96-well microplate, different concentrations of K^+ were added to a 200 nM aptamer solution at room temperature. After incubation for 5 min, 3 μ M PMNT was added (3 μ M monomer unit or 22.7 nM polymer concentration). The fluorescence of PMNT was immediately measured. PMNT was excited at 392 nm and its emission was recorded from 450 nm to 650 nm using a microplate reader (Tecan Spark).

Binding assays of other aptamers. Different concentrations of adenosine, cortisol or caffeine were added into 200 nM corresponding aptamer in 20 mM HEPES, pH 7.5 with 100 mM NaCl and 10 mM $MgCl_2$ at room temperature. After incubation for 5 min, PMNT (3 μ M for adenosine and 5 μ M for cortisol and caffeine) was added. The fluorescence of PMNT was immediately measured after mixing.

SGI fluorescence assay. A 500 μ L reaction solution contained 5 μ M aptamer and $0.5\times$ SGI in 20 mM HEPES, pH 7.5 with 100 mM NaCl and 10 mM $MgCl_2$. Different concentrations of K^+ or cortisol were gradually titrated into the mixture at room temperature. After incubation for 5 min, the fluorescence of SGI was measured with 470 nm excitation and the emission was recorded from 500 nm to 600 nm.

RESULTS AND DISCUSSION

CCP-based K^+ binding assay. In this work, we chose a cationic polythiophene derivative, PMNT (**Figure 1A**), as a model CCP since it showed obvious fluorescence changes in response to the conformational change of DNA.^{40, 41} The average molecular weight of our PMNT was 38 kDa (132 thiophene monomer units) with a molecular weight distribution of 1.87 as characterized by gel permeation chromatography (**Figure S1**). We chose this length since it is much longer than most aptamers (typically between 20 to 60 nucleotides), ensuring more comparable results for different aptamers. As the fluorescence change depends on the length of both CCP and DNA,⁴³ for a short PMNT (e.g. with only 40 repeating units), some aptamers might carry

more charges while others carry less charges compared to the PMNT, resulting in additional variations to the system.

Free PMNT has a random-coiled nonplanar conformation with a fluorescence emission peak at around 530 nm. We first assessed the influence of K^+ on the fluorescence of PMNT, and the fluorescence barely changed after adding 1 mM K^+ (**Figure S2A**). When interacting with a target-free aptamer, electrostatic attraction between the negatively charged aptamer and positively charged PMNT brought them to proximity, stretching PMNT to a highly conjugated conformation with the fluorescence peak redshifted to 580 nm (path A, **Figure 1A**). The addition of K^+ facilitated the formation of a G-quadruplex structure. PMNT could then only wrap around the G-quadruplex resulting in a less conjugated conformation (path B, **Figure 1A**), shifting the fluorescence peak back to 530 nm (**Figure 1B**). Therefore, the fluorescence change of PMNT could reflect aptamer binding to K^+ .

We then evaluated the effect of aptamer concentration. As shown in **Figure S3A**, titration of the K^+ aptamer into 3 μ M PMNT (monomer unit concentration) gradually quenched the 530 nm peak with the maximum quenching effect achieved at 100 nM aptamer. Further increasing the aptamer concentration led to a new peak at 580 nm due to the formation of a highly conjugated, planar conformation of PMNT. We then plotted the fluorescence ratio of 580 nm to 530 nm against the aptamer concentration (**Figure S3B**), from which an apparent dissociation constant (K_d) of 169 nM was obtained. This fluorescence ratio saturated at 500 nM aptamer, and we chose 200 nM aptamer for the K^+ binding assay.

To assess the effect of buffer, we performed our assay in water, Tris-HCl, phosphate buffer (PB) or HEPES (**Figure 1C**). The fluorescence ratio plot showed a K_d of 89 μ M K^+ in water and 336 μ M in Tris-HCl. Using a FRET assay, Takenaka et al. reported a K_d of 280 μ M K^+ for the same aptamer sequence,^{44, 45} which was quite comparable to our results. Therefore, although PMNT is a cationic polymer, it barely interfered with the aptamer (when K^+ and the aptamer were premixed). With lower than 100 μ M K^+ , water also had better sensitivity than Tris-HCl (**Figure S4**). For the other buffers, higher K_d 's of 985 μ M in PB and 2776 μ M in HEPES were obtained. Their higher K_d values were due to the Na^+ ions in PB and HEPES, which competed with K^+ for binding to the aptamer. Thus, we chose water as the optimum reaction medium.

We also switched the order of mixing by incubating PMNT with the aptamer before adding K^+ , where decreased fluorescence was observed in the range of 1 to 100 μ M K^+ , and a shifted fluorescence was achieved with more than 1 mM K^+ (**Figure S5A**). The calculated K_d was 484 μ M (**Figure S5C**), which was 5.4-fold of that from the previous mixing method. When the aptamer and PMNT were premixed, the aptamer needs to be first released from PMNT to bind K^+ . The K_d of the aptamer binding to PMNT was 169 nM (**Figure S3B**), whereas the K_d of the aptamer and K^+ was 89 μ M (**Figure 1C**), demonstrating a tighter binding of the aptamer and PMNT. This is reasonable since the aptamer and PMNT are two polyelectrolytes with strong collective charge attraction. In this case, a correction factor is needed to obtain the true K_d of the aptamer/ K^+ binding, which was similar to that in aptamer strand displacement assays.⁴⁶⁻⁴⁸ A further implication is that the system is

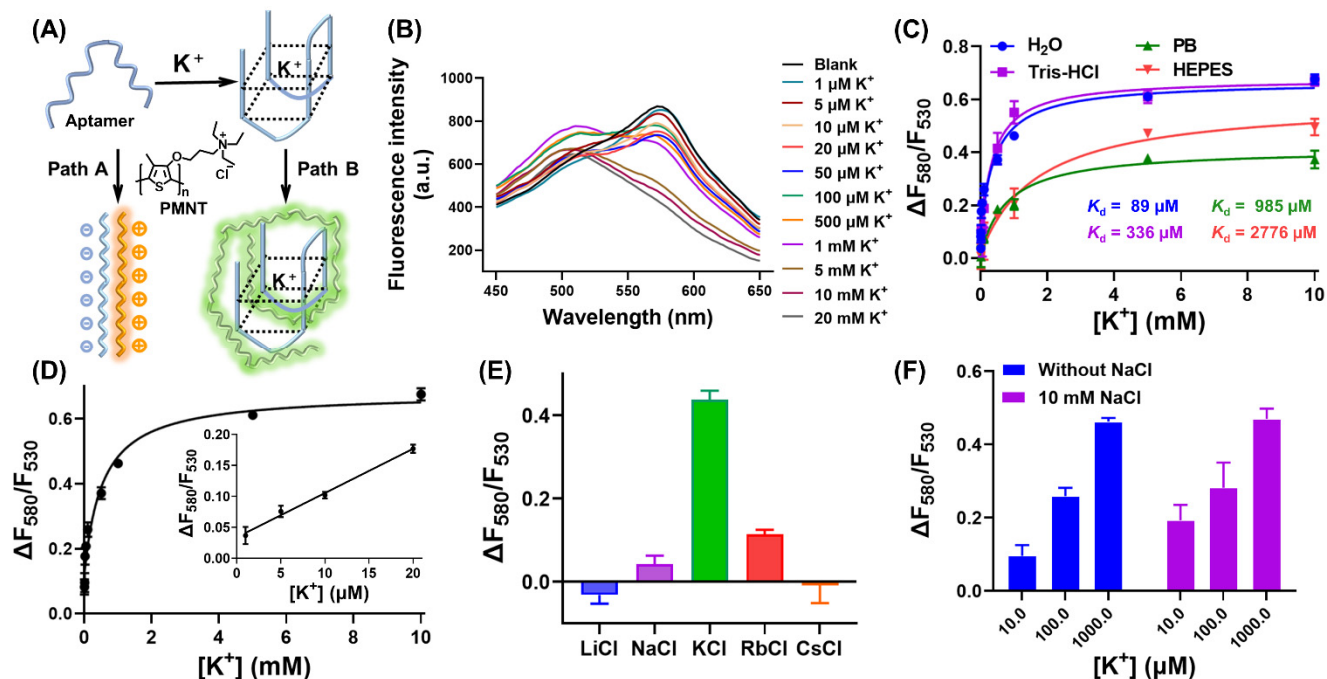


Figure 1. (A) Schematic representation of the CCP-based K^+ binding assay. (B) The fluorescence spectra of PMNT after adding different concentrations of K^+ in 200 nM aptamer in water. (C) The fluorescence ratio of PMNT in response to K^+ concentration in different buffers. (D) The fluorescence ratio of PMNT/aptamer system as a function of K^+ concentration. Inset: the linear response at low K^+ concentrations. (E) The specificity for K^+ detection. The concentration of all of the cations was 1 mM. (F) The detection of K^+ in the presence of 10 mM NaCl. The error bars are standard deviations from triplicate measurements.

under kinetic control, where a binding state reached first would have a kinetic advantage, although the system may not be under the thermodynamic equilibrium. Therefore, we chose to add PMNT after the formation of K^+ /aptamer complex to better reflect aptamer/target binding.

As shown in **Figure 1D**, the fluorescence ratio increased with increasing concentration of K^+ . The fluorescence ratio showed a good linear relationship in the range of 1 μ M to 20 μ M ($R^2 = 0.9675$, inset of **Figure 1D**) with a detection limit of 0.5 μ M. To evaluate the specificity of our CCP-based K^+ binding assay, 1 mM group 1A metals were tested (**Figure 1E**), where only K^+ showed a high signal. In addition, the fluorescence spectrum of K^+ was significantly different from other cations (**Figure S6**). We also measured K^+ in the presence of excess Na⁺. As shown in **Figure 1F**, 10 mM Na⁺ did not affect the response of 0.1 mM or 1 mM K^+ , indicating that our method has high specificity for K^+ .

CCP-based adenosine binding assay. To assess the generality of this method, we then tested a few small molecule targets. Adenosine plays regulatory roles in many cellular processes and it is a model aptamer target.⁴⁹ Addition of 100 μ M adenosine did not affect the fluorescence of PMNT (**Figure S2B**). The adenosine aptamer has a stem-loop structure, and the loop region can stretch PMNT to a highly conjugated conformation (path A, **Figure 2A**). With adenosine, a rigid binding complex similar to a dsDNA was formed.^{17, 50} Thus, PMNT had to unwind the double helix, resulting in a less conjugated structure similar to free PMNT (path B, **Figure 2A**). The conformational change of the aptamer upon target binding may be reflected in the fluorescence change of PMNT.

To control the initial conformation of the aptamer, we varied its terminal stem length from two to six base pairs (bp). As depicted in **Figure S7**, PMNT showed only a small shift to 530 nm after adding adenosine using the 2 bp (Ade-Apt-2) and 4 bp (Ade-Apt-4) aptamers. Only the aptamer with a 6 bp stem (Ade-Apt-6) shifted the fluorescence of PMNT back to 530 nm by adenosine. Therefore, aptamers with a shorter stem are more easily opened, which favored redshift of PMNT fluorescence but disfavored aptamer binding to its target. Therefore, Ade-Apt-6 was chosen for further studies.

We then tested the influence of salt by adding different concentrations of NaCl and MgCl₂. As depicted in **Figure 2B**, 100 mM NaCl was optimal. Too much salt would screen the charge attraction between PMNT and the aptamer, whereas too little salt disfavored aptamer binding. With 100 mM NaCl, we further investigated the influence of MgCl₂ as Mg²⁺ may mediate aptamer-target interactions (**Figure 2C**). The K_d value in the absence of Mg²⁺ was 89 μ M, which decreased to 35 μ M with 2 mM Mg²⁺ and 42 μ M with 10 mM Mg²⁺. A K_d of 42 μ M differed by only a few folds compared to the literature reported value (around 6 to 17 μ M),^{49, 51} suggesting that the interference of PMNT on aptamer binding was minimal. For the subsequent studies, we chose to use 10 mM Mg²⁺.

With the optimal buffer condition (20 mM HEPES, pH 7.5, 100 mM NaCl and 10 mM MgCl₂) and 200 nM Ade-Apt-6, the fluorescence of PMNT at 580 nm first decreased and then shifted to 530 nm with increasing adenosine concentration (**Figure 2D**). Plotting the fluorescence ratio against adenosine concentration (**Figure 2E**), we found that a fine linear relationship in the range of 5 to 80 μ M adenosine ($R^2 = 0.9532$, figure inset) with a detection limit of 1.6 μ M.

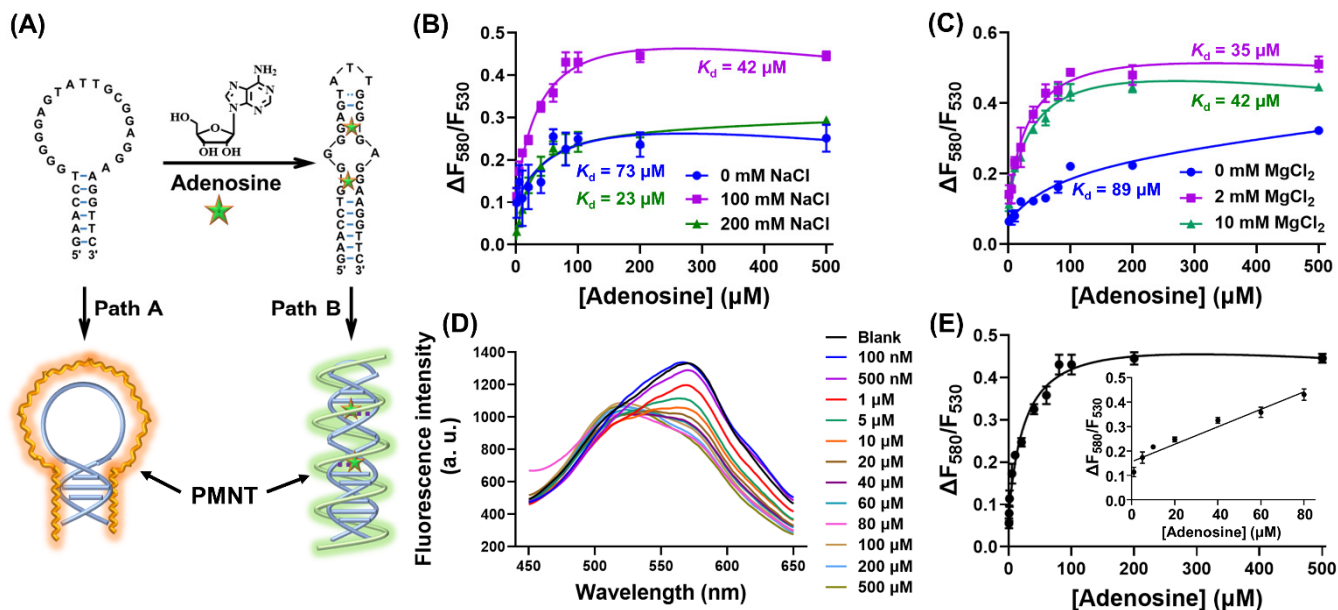


Figure 2. (A) Schematic representation of the CCP-based adenosine binding assay. The fluorescence ratio change of PMNT as a function of adenosine concentration with different concentrations of (B) NaCl and (C) MgCl₂. (D) The fluorescence spectra of PMNT after adding different concentrations of adenosine to 200 nM Ade-Apt-6 aptamer. (E) The correlation of fluorescence ratio of PMNT and adenosine concentration. Inset: linear response at low adenosine concentrations. The error bars are standard deviations from triplicate measurements.

A commonly used dye, SGI, was also used for comparison. As shown in **Figure S8**, the fluorescence of SGI decreased along with increased adenosine concentration, which was consistent with previous reports.¹⁷ While sensitive detection was also achieved, this was a signal-off sensor, whereas the PMNT method allowed ratiometric detection.

We finally assessed the specificity of our method by incubating Ade-Apt-6 with guanosine, cytidine, uridine, AMP, ADP and ATP (**Figure 3A**). AMP, ADP, ATP and adenosine all produced a similar binding signal,⁵² whereas guanosine, cytidine and uridine produced negligible signals, consistent with the literature report (**Figure 3B** and **3C**).¹⁷

CCP-based cortisol binding assay. To further evaluate the generality of our method, we chose a more hydrophobic target, cortisol. Cortisol (50 μM) did not change the fluorescence of PMNT (**Figure S2C**). The cortisol aptamer (CSS.1) has a stable stem-loop secondary structure with a 6 bp stem and two small hairpins were predicted in the loop region (**Figure 4A**).¹⁶ Thus, binding of cortisol may only induce some local conformational changes of the aptamer. We first optimized the aptamer concentration. A higher CSS.1 concentration induced more fluorescence shift of PMNT to 580 nm (**Figure S9**), suggesting that although CSS.1 has a three-way junction structure, it behaved like a ssDNA when interacting with PMNT. We chose 200 nM CSS.1 for subsequent studies.

We then monitored the fluorescence of PMNT/CSS.1 after adding different concentrations of cortisol (**Figure 4B**). While the fluorescence of PMNT at 580 nm gradually dropped, no peak emerged at 530 nm. Therefore, aptamer binding to cortisol did not induce a large conformational change. We reasoned that the aptamer had an irregular three-way junction structure, which behaved like an ssDNA when interacting with PMNT regardless of cortisol binding.

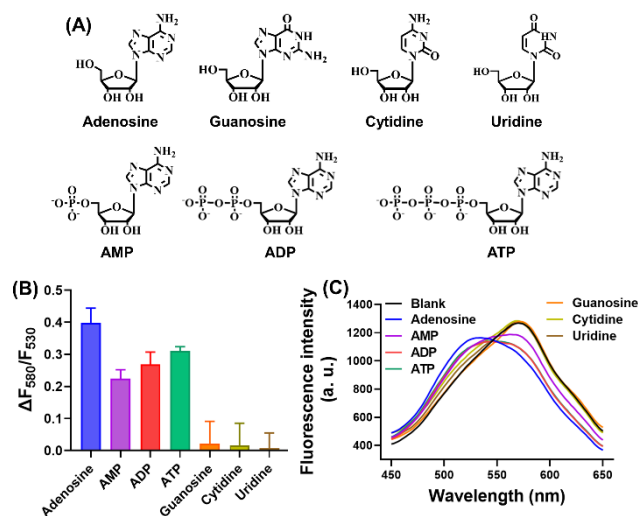


Figure 3. (A) The structures of the adenosine analogues tested in this work. (B) The specificity test with 100 μM competing molecules. The error bars are standard deviations from triplicate measurements. (C) The fluorescence spectra of PMNT after adding the adenosine analogues to 200 nM Ade-Apt-6.

We also assessed the effect of salt on the cortisol aptamer (**Figure S10**). This aptamer was insensitive to the concentration of NaCl, although the binding of CSS.1 and cortisol was promoted by Mg²⁺, which was consistent with a previous report.¹⁶ The effect of Mg²⁺ saturated at 10 mM. We then studied the effect of aptamer stem length. CSS.1 with a shorter stem may undergo a larger conformational change after binding with cortisol. Under the optimized buffer condition (20 mM HEPES, pH 7.5 with 100 mM NaCl and 10 mM MgCl₂), we tested three truncated CSS.1 aptamers. As shown in **Figure 4C**, when the stem was less than 4 bp, very little fluorescence change was

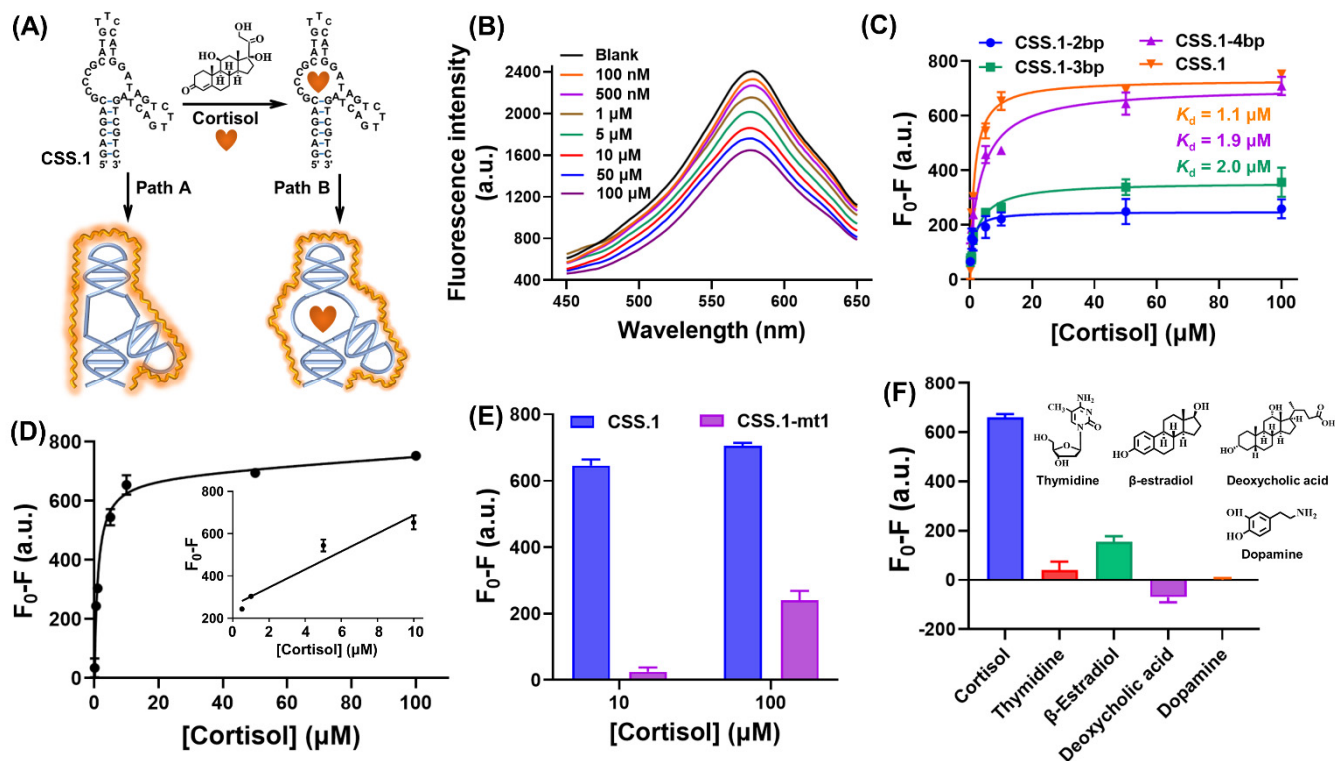


Figure 4. (A) Schematic representation of the CCP-based cortisol binding assay. (B) The fluorescence spectra of PMNT after adding different concentrations of cortisol to 200 nM CSS.1. (C) The fluorescence intensity change of PMNT in response to cortisol concentration using aptamers of different stem lengths. (D) The correlation between the fluorescence intensity change and cortisol concentration. Inset: linear response at low cortisol concentrations. (E) A control with the nonbinding CSS.1 mutant. (F) The specificity test with 10 μM cortisol analogues. The error bars are standard deviations from triplicate measurements.

produced, and the fluorescence difference increased with longer stems. The original CSS.1 with a 6 bp stem generated the largest fluorescence difference with a K_d of 1.1 μM . This K_d value was very close to the K_d measured by ITC (0.7 μM),¹⁶ verifying that PMNT showed very little interference on aptamer binding.

We also assessed the fluorescence change of PMNT by mixing PMNT with aptamer before adding cortisol. This sample showed less fluorescence changes compared to adding PMNT to the cortisol/CSS.1 complex (Figure S5B). The calculated K_d was 2.9 μM (Figure S5D) which was 2.8-fold of previous mixing method. This was also consistent with the observation of the K^+ aptamer shown above.

The cortisol binding assay was then assessed. As shown in Figure 4B and 4D, the fluorescence intensity showed a good linear relationship in the range of 1 to 10 μM cortisol ($R^2=0.9226$) with a detection limit of 0.2 μM . We also compared our method with the SGI staining method (Figure S11A and B). Interestingly, SGI could only detect cortisol higher than 1 μM using 5 μM CSS.1. With 1 μM CSS.1, the fluorescence spectra showed little response to cortisol concentration (Figure S11C). To directly compare the sensitivity of the two methods, we plotted the percentage of fluorescence change in response to cortisol concentration (Figure S11D and E). The sensitivity of PMNT was 1.3-fold of SGI.

As a further control, a nonbinding mutated was tested, which differs from CSS.1 by only two bases (the underlined bases in Table S1). As shown in Figure 4E, the fluorescence of the mutant was changed very little upon adding cortisol, confirming specific aptamer binding. We then assessed the specificity using thymidine, β -estradiol, deoxycholic acid and dopamine and none of them showed a response (Figure 4F).

CCP-based caffeine binding assay. As a final example, a caffeine aptamer named CAFF203 was tested.⁵³ The fluorescence of PMNT was almost unchanged after adding 50 μM caffeine (Figure S2C). CAFF203 also has an internal rigid hairpin and it binds caffeine in a similar way as the cortisol aptamer (Figure 5A). Indeed, upon adding caffeine, this aptamer only showed decreased 580 nm peak without shifting the peak back to 530 nm. Aptamers with a longer stem ensured a higher binding affinity (Figure 5B), consistent with the adenosine and cortisol aptamers. The fluorescence gradually dropped with increasing concentration of caffeine (Figure 5C and 5D) and caffeine could be quantified in the range of 1 to 10 μM with a detection limit of 0.4 μM (Figure 5E). The specific binding of CAFF203 to caffeine rather than paraxanthine, theobromine and theophylline was also shown (Figure 5F). Therefore, PMNT can also reflect the binding of the caffeine aptamer.

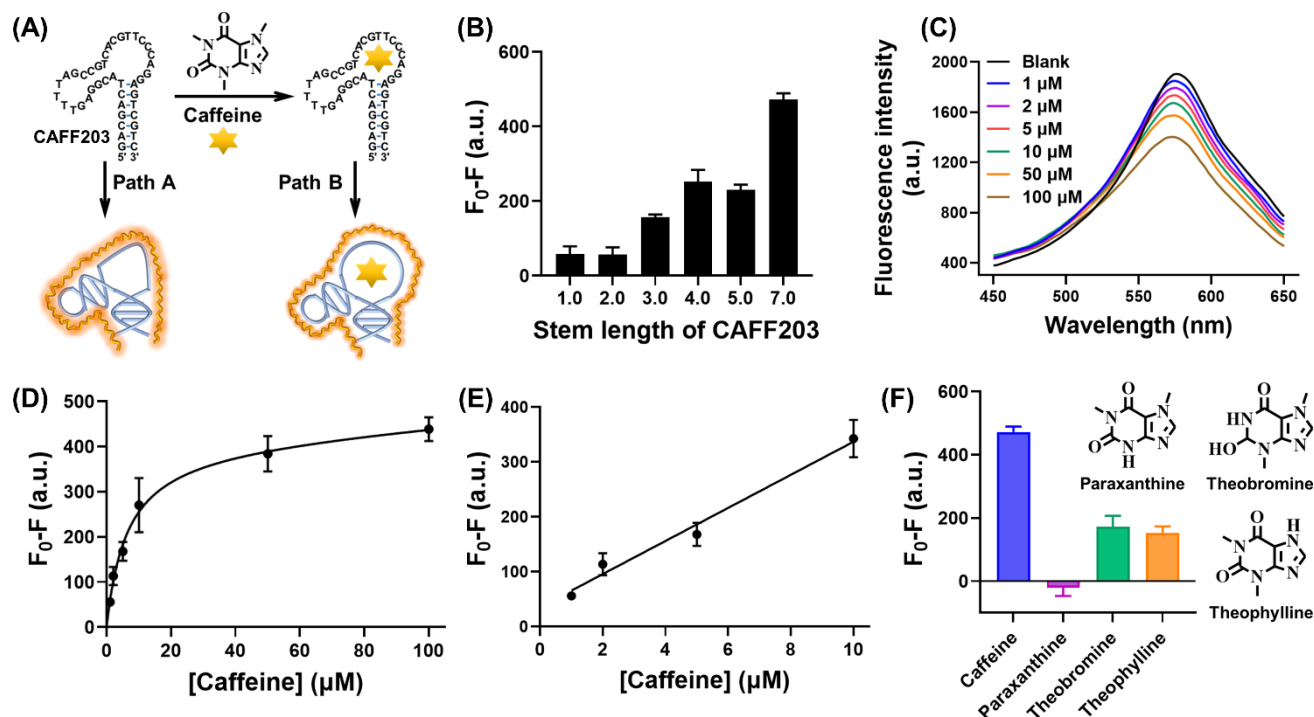


Figure 5. (A) Schematic representation of the CCP-based caffeine binding assay. (B) The fluorescence intensity change of PMNT in response to caffeine concentration using aptamers with different stem lengths. (C) The fluorescence spectra of PMNT after adding different concentrations of caffeine to 200 nM CAFF203. (D) The correlation between the fluorescence intensity change and caffeine concentration. (E) The linear response at low caffeine concentrations. (F) The specificity test with 100 μM analogues. The error bars are standard deviations from triplicate measurements.

Discussion on different types of aptamers. In the four aptamers we tested in this work, they all showed target-dependent fluorescence change. The CCP-based fluorescent binding assay can be summarized to a few types as shown in **Figure 6**. First, some aptamers have little initial secondary structure, but can fold into a rigid structure upon target binding. Examples of this type include formation of G-quadruplex and DNA hybridization (path I, **Figure 6**). For them, an obviously shifted fluorescence peak of PMNT from 580 nm to 530 nm upon target binding can be observed. Although the adenosine aptamer has a simple stem-loop structure, the initial structureless loop can render its interaction with PMNT like an ssDNA. After binding adenosine, the structure rigidified to be similar to a duplex DNA. So, it also belongs to this type. The second type is represented by the cortisol and caffeine aptamers (path II, **Figure 6**). They have a branched but rigid initial structure, which did not change much after target binding. Their interaction with PMNT is closer to a ssDNA regardless of target binding as reflected by the retained 580 nm peak after adding target molecules.

Based on the above discussion, there could be another two potential types (path III and IV, **Figure 6**), where a target-free aptamer has a 530 nm emission peak. This requires the initial structure to be already rigid and duplex like. So far, we have not found such an example.

Based on the wavelength change and the classification in **Figure 6**, we can in turn deduce some structural information about aptamer binding. This is an advantage compared to the SGI based assays. We believe the fluorescence PMNT can be used as general aptamer binding assay. In addition, some assays might also be useful as fluorescent biosensors, especially those with a fluorescence peak shift allowing ratiometric detection.

Based on the data we collected so far, for stem-loop structured aptamers, a longer stem is more favorable for the signal change of PMNT. This has been observed in **Figure 4C, 5B** and **S4**. In addition, salt concentration is an important factor and they can affect K_d values. For small molecules, a typical buffer close to physiological salt concentration is a good starting point. The K_d measured is likely to be different from the real K_d of aptamers since PMNT may act as a competitor. Based on the examples presented in this work, the difference is not very large, especially when the aptamer and target are mixed first. For example, the K_d for adenosine was measured to be around 6 μM based on analytical ultrafiltration and 16.4 μM using ITC.^{49, 52} Our method obtained a K_d of 42 μM which showed only several fold differences (**Figure 2B** and **2C**). Also, the K_d for cortisol was 0.7 μM by ITC,¹⁶ and our method achieved a similar K_d of 1.1 μM (**Figure 4C**).

We made some comparisons with SGI in this work. Fundamentally, SGI and other dyes probe local structures of DNA, whereas PMNT probes global structures. This is a fundamental difference between using DNA staining dyes and CCP. Our PMNT showed either a similar performance or even better responses than SGI, indicating the advantage of probing global aptamer structures for developing binding assays.

CONCLUSIONS

In this work, we demonstrated a general CCP-based fluorescent binding assay for small molecule targets including K^+ , adenosine, cortisol and caffeine. The conformational change of aptamers upon target binding was reflected in the fluorescence of PMNT. Although PMNT competes with target for aptamer binding, our method achieved similar K_d compared with other commonly used methods, as long as aptamers and targets were

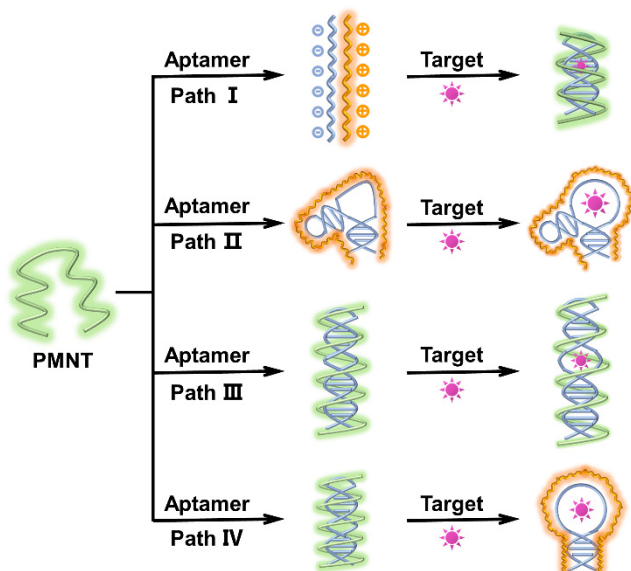


Figure 6. Schematic representation of the different types of the CCP-based fluorescence binding assay. The blue lines are for aptamers, green lines for random PMNT with 530 nm fluorescence peak, and orange lines for rigid conformational PMNT with 580 nm fluorescence peak.

mixed before adding PMNT. In addition, for aptamers with a stem-loop structure, a longer stem promoted more fluorescence change of PMNT. This method also retained the high specificity of the aptamers. Based on the shift of the fluorescence peak, the structural of aptamers before and after target binding can be deduced. The utilization of biocompatible CCPs and non-labeled aptamer ensures our assay to be a simple, label-free, and cost-effective method, which is practical to assess aptamer binding affinity and shows a great potential as general label-free fluorescent biosensors.^{54, 55}

ASSOCIATED CONTENT

Supporting Information

The Supporting Information is available free of charge on the ACS Publications website.

The GPC characterization of PMNT, the optimization of reaction conditions, such as aptamer concentration, stem length of aptamers, NaCl and MgCl₂ concentration, the detection of 5-100 μM K⁺ in water and Tris-HCl, the detection of K⁺ with other interfering cations, the detection of target using SGI-based staining method, and the sequences of aptamers used in this work (PDF)

AUTHOR INFORMATION

Corresponding Author

*Juewen Liu – Department of Chemistry, Waterloo Institute for Nanotechnology, University of Waterloo, Waterloo N2L 3G1 Ontario, Canada; orcid.org/0000-0001-5918-9336; Email: liujw@uwaterloo.ca

*Zhengping Li - School of Chemistry and Biological Engineering, University of Science and Technology Beijing, Beijing, 100083, China; orcid.org/0000-0002-7573-8822; Email: lzxbd@ustb.edu.cn

Author Contributions

The manuscript was written through contributions of all authors. All authors have given approval to the final version of the manuscript.

Notes

There are no conflicts to declare.

ACKNOWLEDGMENT

Funding for this work was from the Natural Sciences and Engineering Research Council of Canada (NSERC), the International Exchange Growth Program for Young Teachers (QNXM20220051) and the Fundamental Research Funds for the Central Universities (FRF-IDRY-20-026). P. Zhang was supported by a China Scholarship Council (CSC) scholarship to visit the University of Waterloo.

REFERENCES

- (1) Yoshikawa, A. M.; Wan, L.; Zheng, L.; Eisenstein, M.; Soh, H. T. A system for multiplexed selection of aptamers with exquisite specificity without counterselection. *Proc. Natl. Acad. Sci. U. S. A.* **2022**, *119*, e2119945119.
- (2) Yu, H.; Alkhamis, O.; Canoura, J.; Liu, Y.; Xiao, Y. Advances and challenges in small - molecule DNA aptamer isolation, characterization, and sensor development. *Angew. Chem. Int. Ed.* **2021**, *60*, 16800-16823.
- (3) Li, L.; Xu, S.; Yan, H.; Li, X.; Yazd, H. S.; Li, X.; Huang, T.; Cui, C.; Jiang, J.; Tan, W. Advances and challenges in small-molecule DNA aptamer isolation, characterization, and sensor development. *Angew. Chem., Int. Ed.* **2021**, *60*, 2221-2231.
- (4) Liu, M.; Yin, Q.; Chang, Y.; Zhang, Q.; Brennan, J. D.; Li, Y. In vitro selection of circular DNA aptamers for biosensing applications. *Angew. Chem., Int. Ed.* **2019**, *58*, 8013-8017.
- (5) Wu, X.; Liu, H.; Han, D.; Peng, B.; Zhang, H.; Zhang, L.; Li, J.; Liu, J.; Cui, C.; Fang, S. Elucidation and structural modeling of CD71 as a molecular target for cell-specific aptamer binding. *J. Am. Chem. Soc.* **2019**, *141*, 10760-10769.
- (6) Nakatsuka, N.; Yang, K.-A.; Abendroth, J. M.; Cheung, K. M.; Xu, X.; Yang, H.; Zhao, C.; Zhu, B.; Rim, Y. S.; Yang, Y.; Weiss, P. S.; Stojanovic, M. N.; Andrews, A. M. Aptamer-field-effect transistors overcome Debye length limitations for small-molecule sensing. *Science* **2018**, *362*, 319-324.
- (7) Batey, R. T.; Gilbert, S. D.; Montagne, R. K. Structure of a natural guanine-responsive riboswitch complexed with the metabolite hypoxanthine. *Nature* **2004**, *432*, 411-415.
- (8) Zong, C.; Liu, J. The arsenic-binding aptamer cannot bind arsenic: critical evaluation of aptamer selection and binding. *Anal. Chem.* **2019**, *91*, 10887-10893.
- (9) Bottari, F.; Daems, E.; de Vries, A.-M.; Van Wielendaele, P.; Trashin, S.; Blust, R.; Sobott, F.; Madder, A.; Martins, J. C.; De Wael, K. Do Aptamers Always Bind? The Need for a Multifaceted Analytical Approach When Demonstrating Binding Affinity between Aptamer and Low Molecular Weight Compounds. *J. Am. Chem. Soc.* **2020**, *142*, 19622-19630.
- (10) Zhao, Y.; Yavari, K.; Liu, J. Critical evaluation of aptamer binding for biosensor designs. *TrAC, Trends Anal. Chem.* **2022**, *146*, 116480.
- (11) McKeague, M.; Calzada, V.; Cerchia, L.; DeRosa, M.; Heemstra, J. M.; Janjic, N.; Johnson, P. E.; Kraus, L.; Limson, J.; Mayer, G.; Nilsen-Hamilton, M.; Porciani, D.; Sharma, T. K.; Suess, B.; Tanner, J. A.; Shigdar, S. The minimum aptamer publication standards (MAPS guidelines) for de novo aptamer selection. *Aptamers* **2022**, *6*, 10-18.
- (12) McKeague, M.; De Girolamo, A.; Valenzano, S.; Pascale, M.; Ruscito, A.; Velu, R.; Frost, N. R.; Hill, K.; Smith, M.; McConnell, E. M.; DeRosa, M. C. Comprehensive analytical comparison of strategies used for small molecule aptamer evaluation. *Anal. Chem.* **2015**, *87*, 8608-8612.
- (13) Canoura, J.; Yu, H.; Alkhamis, O.; Roncancio, D.; Farhana, R.; Xiao, Y. Accelerating post-SELEX aptamer engineering using exonuclease digestion. *J. Am. Chem. Soc.* **2020**, *143*, 805-816.

- (14) Yang, L.; Yin, X.; An, B.; Li, F. Precise Capture and Direct Quantification of Tumor Exosomes via a Highly Efficient Dual-Aptamer Recognition-Assisted Ratiometric Immobilization-Free Electrochemical Strategy. *Anal. Chem.* **2021**, *93*, 1709-1716.
- (15) Wang, X.; Yang, Y.; Yin, Y.; Zeng, N.; Dong, Y.; Liu, J.; Wang, L.; Yang, Z.; Yang, C. High-Throughput Aptamer Microarrays for Fluorescent Detection of Multiple Organophosphorus Pesticides in Food. *Anal. Chem.* **2022**, *94*, 3173-3179.
- (16) Niu, C.; Ding, Y.; Zhang, C.; Liu, J. Comparing two cortisol aptamers for label-free fluorescent and colorimetric biosensors. *Sens. Diagn.* **2022**, *1*, 541-549.
- (17) Li, Y.; Liu, B.; Huang, Z.; Liu, J. Engineering base-excised aptamers for highly specific recognition of adenosine. *Chem. Sci.* **2020**, *11*, 2735-2743.
- (18) Xu, C.; He, X.; Peng, Y.; Dai, B.; Liu, B.; Cheng, S. Facile strategy to enhance specificity and sensitivity of molecular beacons by an aptamer-functionalized delivery vector. *Anal. Chem.* **2020**, *92*, 2088-2096.
- (19) Qiu, L.; Wu, C.; You, M.; Han, D.; Chen, T.; Zhu, G.; Jiang, J.; Yu, R.; Tan, W. A targeted, self-delivered, and photocontrolled molecular beacon for mRNA detection in living cells. *J. Am. Chem. Soc.* **2013**, *135*, 12952-12955.
- (20) Nutiu, R.; Li, Y. Structure-switching signaling aptamers. *J. Am. Chem. Soc.* **2003**, *125*, 4771-4778.
- (21) Nutiu, R.; Mei, S.; Liu, Z.; Li, Y. Engineering DNA aptamers and DNA enzymes with fluorescence-signaling properties. *Pure Appl. Chem.* **2004**, *76*, 1547-1561.
- (22) Hartig, J. S.; Najafi-Shoushtari, S. H.; Grüne, I.; Yan, A.; Ellington, A. D.; Famulok, M. Protein-dependent ribozymes report molecular interactions in real time. *Nat. Biotechnol.* **2002**, *20*, 717-722.
- (23) Billet, B.; Chovelon, B.; Fiore, E.; Oukacine, F.; Petrillo, M. A.; Faure, P.; Ravelet, C.; Peyrin, E. Aptamer Switches Regulated by Post-Transition/Transition Metal Ions. *Angew. Chem., Int. Ed.* **2021**, *133*, 12454-12458.
- (24) Deng, B.; Lin, Y.; Wang, C.; Li, F.; Wang, Z.; Zhang, H.; Li, X.-F. Le, X. C. Aptamer binding assays for proteins: the thrombin example—a review. *Anal. Chim. Acta* **2014**, *837*, 1-15.
- (25) Lu, C.; Jimmy Huang, P. J.; Zheng, J.; Liu, J. 2-Aminopurine Fluorescence spectroscopy for probing a glucose binding aptamer. *ChemBioChem* **2022**, *23*, e202200127.
- (26) Thevendran, R.; Citartan, M. Assays to estimate the binding affinity of aptamers. *Talanta* **2022**, *238*, 122971.
- (27) Saha, K.; Agasti, S. S.; Kim, C.; Li, X.; Rotello, V. M. Gold nanoparticles in chemical and biological sensing. *Chem. Rev.* **2012**, *112*, 2739-2779.
- (28) Yazdian-Robati, R.; Hedayati, N.; Ramezani, M.; Abnous, K.; Taghdisi, S. M. Colorimetric gold nanoparticles-based aptasensors. *Nanomed. J.* **2018**, *5*, 1-5.
- (29) Liu, J.; Cao, Z.; Lu, Y. Functional nucleic acid sensors. *Chem. Rev.* **2009**, *109*, 1948-1998.
- (30) Liu, B.; Liu, J. Interface-driven hybrid materials based on DNA-functionalized gold nanoparticles. *Matter* **2019**, *1*, 825-847.
- (31) Li, H.; Rothberg, L. Colorimetric detection of DNA sequences based on electrostatic interactions with unmodified gold nanoparticles. *Proc. Natl. Acad. Sci. U.S.A.* **2004**, *101*, 14036-14039.
- (32) Li, H.; Rothberg, L. J. Label-Free Colorimetric Detection of Specific Sequences in Genomic DNA Amplified by the Polymerase Chain Reaction. *J. Am. Chem. Soc.* **2004**, *126*, 10958-10961.
- (33) Zhang, F.; Huang, P. J. J.; Liu, J. Sensing adenosine and ATP by aptamers and gold nanoparticles: opposite trends of color change from domination of target adsorption instead of aptamer binding. *ACS Sens.* **2020**, *5*, 2885-2893.
- (34) Feng, X.; Liu, L.; Wang, S.; Zhu, D. Water-soluble fluorescent conjugated polymers and their interactions with biomacromolecules for sensitive biosensors. *Chem. Soc. Rev.* **2010**, *39*, 2411-2419.
- (35) Zhou, L.; Lv, F.; Liu, L.; Wang, S. Water-soluble conjugated organic molecules as optical and electrochemical materials for interdisciplinary biological applications. *Acc. Chem. Res.* **2019**, *52*, 3211-3222.
- (36) Kim, B.; Jung, I. H.; Kang, M.; Shim, H. K.; Woo, H. Y. Cationic conjugated polyelectrolytes-triggered conformational change of molecular beacon aptamer for highly sensitive and selective potassium ion detection. *J. Am. Chem. Soc.* **2012**, *134*, 3133-3138.
- (37) He, F.; Tang, Y.; Wang, S.; Li, Y.; Zhu, D. Fluorescent amplifying recognition for DNA G-quadruplex folding with a cationic conjugated polymer: a platform for homogeneous potassium detection. *J. Am. Chem. Soc.* **2005**, *127*, 12343-12346.
- (38) Ho, H. A.; Leclerc, M. Optical sensors based on hybrid aptamer/conjugated polymer complexes. *J. Am. Chem. Soc.* **2004**, *126*, 1384-1387.
- (39) Liu, X.; Tang, Y.; Wang, L.; Zhang, J.; Song, S.; Fan, C.; Wang, S. Optical detection of mercury (II) in aqueous solutions by using conjugated polymers and label-free oligonucleotides. *Adv. Mater.* **2007**, *19*, 1471-1474.
- (40) Ho, H. A.; Boissinot, M.; Bergeron, M. G.; Corbeil, G.; Doré, K.; Boudreau, D.; Leclerc, M. Colorimetric and fluorometric detection of nucleic acids using cationic polythiophene derivatives. *Angew. Chem., Int. Ed.* **2002**, *114*, 1618-1621.
- (41) Zhang, P.; Lu, C.; Niu, C.; Wang, X.; Li, Z.; Liu, J. Binding Studies of Cationic Conjugated Polymers and DNA for Label-Free Fluorescent Biosensors. *ACS Appl. Polym. Mater.* **2022**, *4*, 6211-6218.
- (42) Tang, Y.; Feng, F.; He, F.; Wang, S.; Li, Y.; Zhu, D. Direct visualization of enzymatic cleavage and oxidative damage by hydroxyl radicals of single-stranded DNA with a cationic polythiophene derivative. *J. Am. Chem. Soc.* **2006**, *128*, 14972-14976.
- (43) Wang, S.; Liu, B.; Gaylord, B. S.; Bazan, G. C. Size-specific interactions between single- and double-stranded oligonucleotides and cationic water-soluble oligofluorenes. *Adv. Funct. Mater.* **2003**, *13*, 463-467.
- (44) Ueyama, H.; Takagi, M.; Takenaka, S. A Novel Potassium Sensing in Aqueous Media with a Synthetic Oligonucleotide Derivative. Fluorescence Resonance Energy Transfer Associated with Guanine Quartet-Potassium Ion Complex Formation. *J. Am. Chem. Soc.* **2002**, *124*, 14286-14287.
- (45) Takenaka, S.; Juskowiak, B. Fluorescence detection of potassium ion using the G-quadruplex structure. *Anal. Sci.* **2011**, *27*, 1167-1167.
- (46) Hu, J.; Easley, C. J., A Simple and Rapid Approach for Measurement of Dissociation Constants of DNA Aptamers against Proteins and Small Molecules Via Automated Microchip Electrophoresis. *Analyst* **2011**, *136*, 3461-3468.
- (47) Yang, K.-A.; Chun, H.; Zhang, Y.; Pecic, S.; Nakatsuka, N.; Andrews, A. M.; Worgall, T. S.; Stojanovic, M. N., High-Affinity Nucleic-Acid-Based Receptors for Steroids. *ACS Chem. Biol.* **2017**, *12*, 3103-3112.
- (48) Huang, P. J. J.; Liu, J. A DNA Aptamer for Theophylline with Ultrahigh Selectivity Reminiscent of the Classic RNA Aptamer. *ACS Chem. Biol.* **2022**, *17*, 2121-2129.
- (49) Huizenga, D. E.; Szostak, J. W. A DNA aptamer that binds adenosine and ATP. *Biochemistry* **1995**, *34*, 656-665.
- (50) Biniuri, Y.; Albada, B.; Willner, I. Probing ATP/ATP-aptamer or ATP-aptamer mutant complexes by microscale thermophoresis and molecular dynamics simulations: discovery of an ATP-aptamer sequence of superior binding properties. *J. Phys. Chem. B* **2018**, *122*, 9102-9109.
- (51) Zhang, Z.; Oni, O.; Liu, J. New insights into a classic aptamer: binding sites, cooperativity and more sensitive adenosine detection. *Nucleic Acids Res.* **2017**, *45*, 7593-7601.
- (52) Li, Y.; Liu, J. Aptamer-based strategies for recognizing adenine, adenosine, ATP and related compounds. *Analyst* **2020**, *145*, 6753-6768.
- (53) Huang, P. J. J.; Liu, J. Selection of aptamers for sensing caffeine and discrimination of its three single demethylated analogues. *Anal. Chem.* **2022**, *94*, 3142-3149.
- (54) Li, J.; Mo, L.; Lu, C.-H.; Fu, T.; Yang, H.-H.; Tan, W., Functional Nucleic Acid-Based Hydrogels for Bioanalytical and Biomedical Applications. *Chem. Soc. Rev.* **2016**, *45*, 1410-1431.
- (55) Li, Y.; Gao, H.; Qi, Z.; Huang, Z.; Ma, L.; Liu, J., Freezing-Assisted Conjugation of Unmodified Diblock DNA to Hydrogel Nanoparticles and Monoliths for DNA and Hg²⁺ Sensing. *Angew. Chem. Int. Ed.* **2021**, *60*, 12985-12991.

For TOC Figure Only

